Paper for the 53rd Structures, Structural Dynamics, and Materials Conference:
Special Sessions on Nanostructured Materials

Multiscale Modeling of Structurally-Graded Materials Using Discrete Dislocation Plasticity Models and Continuum Crystal Plasticity Models

E. Saether[*], J.D. Hochhalter[†] and E. H. Glaessgen[‡]
Durability, Damage Tolerance and Reliability Branch
NASA Langley Research Center, Hampton, Virginia, 23681

A multiscale modeling methodology that combines the predictive capability of discrete dislocation plasticity and the computational efficiency of continuum crystal plasticity is developed. Single crystal configurations of different grain sizes modeled with periodic boundary conditions are analyzed using discrete dislocation plasticity (DD) to obtain grain size-dependent stress-strain predictions. These relationships are mapped into crystal plasticity parameters to develop a multiscale DD/CP model for continuum level simulations. A polycrystal model of a structurally-graded microstructure is developed, analyzed and used as a benchmark for comparison between the multiscale DD/CP model and the DD predictions. The multiscale DD/CP model follows the DD predictions closely up to an initial peak stress and then follows a strain hardening path that is parallel but somewhat offset from the DD predictions. The difference is believed to be from a combination of the strain rate in the DD simulation and the inability of the DD/CP model to represent non-monotonic material response.

Introduction

Nanocrystalline metallic materials have been developed over the past several decades with the promise of achieving higher strengths than are possible with traditional microstructures (Gleiter, 1989). Despite the advantage of increased strength, the long-studied disadvantages of nanocrystalline metals include their lack of ductility and their low fracture toughness (Whang, 2011). To address these shortcomings, a microstructural concept as shown in Figure 1, that offers the promise of combining the strength of nanocrystalline metals with the ductility and toughness of traditional metals was developed by Fang and co-workers (Fang, 2011). These structurally-graded metallic materials consist of two or more layers in which the grain size varies from relatively fine (nanometers to hundreds of nanometers) to relatively coarse (microns to tens of microns). The layered structure is analogous to a laminated polymeric composite material, but here, the finer grains contribute much of the overall material strength while the coarser grains contribute much of the ductility and toughness. Such layered structures may offer the ability to simultaneously optimize strength and ductility within a single engineered microstructure.

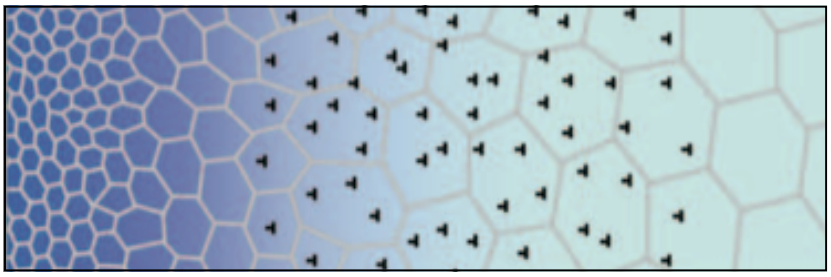

Figure 1: Structurally-graded microstructural configuration (Fang, 2011).

[*] Senior Aerospace Engineer, AIAA Member
[†] Aerospace Engineer, AIAA Member
[‡] Assistant Branch Head, AIAA Associate Fellow

These emerging material forms motivate the development of new computational materials modeling methods that can address their unique microstructural configurations and responses. Because of the small grain sizes considered, analyses that are developed for structurally-graded materials must be able to predict length scale effects. In addition to the well-known effects of grain size on material response in a gradient field (see, for example, Fleck, 1994), recent experimental studies (Uchic, 2009) have revealed that a grain-size dependence can also exist in the absence of gradients. As discussed in Uchic (2009), Uchic and others have used in-situ compression studies of micropillar specimens with characteristic dimensions in the range from less than a micron to tens of microns to evaluate material flow properties and the dependence of dislocation process on grain size.

The dynamic evolution of lattice defects that are described by a multitude of dislocation mechanisms constitutes the atomistic basis for plastic deformation, toughness and strain hardening in metallic microstructures. Short-range interactions are described by local constitutive laws in which dislocations can annihilate, generate pile-ups, combine through complex junction formation, or become pinned to function as Frank-Read sources for nucleating additional dislocations on associated slip planes. These interactions dictate the initiation of yielding, subsequent strain hardening and development of internal structures such as shear bands, sub-cells and low-angle grain boundaries (Hull and Bacon, 2001).

Dislocations can be simulated in either a discrete or homogenized sense. Among the methods that have been developed to simulate dislocations in a discrete sense are molecular dynamics (MD) and discrete dislocation plasticity (DD). Molecular dynamics (MD) is the obvious computational approach for domains that are on the order of nanometers or tens of nanometers. MD has been used to simulate the most fundamental mechanisms of deformation and to calibrate energy and strength parameters for larger scale analyses (see, for example, Yamakov, 2006; Yamakov, 2009; Warner, 2007). However, domains in the size range from hundreds of nanometers to microns are (currently) too large for a systematic study using MD. Thus, DD simulations have been developed to approximate the complex evolution of dislocation fields using idealized representations of the interactions between individual dislocations (Van der Giessen, 1995; Needleman, 2001).

At even larger length scales, enhanced continuum plasticity methods have been developed to simulate the collective response of large aggregates of dislocations as continuum analogues to discrete MD or DD methods wherein a sufficient volume of material is considered to permit homogenization of the underlying deformation processes. These methods include strain gradient plasticity (SGP) which includes a material length scale enabling an approximation of material size effects, crystal plasticity (CP) which includes an implicit representation of plastic slip systems and strain gradient crystal plasticity (SGCP) which addresses both material size effects and plastic slip on individual slip systems (Roters, 2010; Evans, 2009; Fleck, 1997; Hutchinson, 2000; Han, 2005a; Han, 2005b).

Sequential multiscale modeling approaches enable the development of hybrid analyses wherein insightful but computationally intensive discrete methods are integrated with computationally efficient continuum methods (Saether, 2009). The multiscale modeling method developed in the present work integrates two-dimensional discrete dislocation plasticity with continuum crystal

plasticity using an inverse modeling approach. The DD analysis is used to determine the size-dependent stress-strain response of individual grains by modeling the formation of dislocations and determining their interactions with other dislocations, with distributed obstacles within the grain domain, and with the outer grain boundaries (GBs). Information is then homogenized as an effective stress-strain response and mapped into a reduced set of parameters for a crystal plasticity analysis of material response.

Because of the generality of the inverse approach, there are typically several sets of optimized crystal plasticity parameters that minimize the error represented by an objective function. Consequently, mechanics-based arguments are then made to select a single meaningful set of parameters that fully define the DD-informed CP constitutive model, hereafter referred to as the "DD/CP model." In the present study, the DD/CP model is applied to simulate plastic deformation in a structurally-graded material wherein local grain size varies from 100 nm to 2 microns in distinct layers.

This paper is composed of the following sections. First, the discrete dislocation plasticity and continuum crystal plasticity analyses are presented. Second, the inverse formulation is described, along with the CP parameters that were optimized to reproduce the DD results. Third, results of a verification problem are discussed, where the stress-strain behavior of a structurally-graded polycrystal is predicted separately using DD simulation and the DD/CP model. Finally, a brief summary is presented.

Discrete Dislocation Plasticity and Continuum Crystal Plasticity

Discrete Dislocation Plasticity Formulation and Results

Discrete dislocation plasticity simulations may be performed in either two or three dimensions. In two-dimensional simulations, dislocations are represented as point defects that are constrained to move along particular slip planes. The result is a simplified representation that simulates dislocation interaction and the resulting plastic and hardening behavior of material domains. Benzerga (2004) has advanced the representation of three-dimensional mechanisms such as junction formation, dynamic sources and shearable obstacles in the form of two-dimensional analogues. These analogues have been incorporated into the present analysis. While the inelastic stress-strain and hardening behavior is a main outcome of the analysis, much investigation has also been performed to determine the formation of dislocation structures such as sub-cells, shear bands and low-angle grain boundaries (Devincre, 2001; Mughrabi, 1983; Thomson, 2002). These internal structures are related to the material plastic response and, due to constraints on dislocation mobility, result in hardening or increased toughness of the material.

The size of grains in a metallic microstructure has important consequences on overall material behavior, whereby ductility tends to increase and yield stress tends to decrease with increasing grain size (Freidman, 1998; Zhu, 2006). The dependence of yield stress on grain dimension is described by the Hall-Petch relation (Hall, 1951; Petch, 1953). Other grain size-dependent deformation mechanisms (Evers, 2002; Gavriljuk, 1999; Li, 1970) have been observed and are implicitly considered in the present DD simulation, including:

- Dislocation pile-up: Decreasing grain size causes the number of dislocations piling-up against a grain boundary to be reduced. As a result, the stress concentration at the grain boundary is lowered which lessens nucleation of new dislocations in the neighboring grain.
- Reduction in slip magnitude: Decreasing grain size reduces the mean free path for dislocations and results in higher strength with reduced ductility.
- Constrained nucleation: Decreasing grain size causes a reduction in the overall production of dislocations, most of which nucleate along grain boundaries. This contrasts with the high availability of Frank-Read sources in larger grains that permit less constrained dislocation generation and associated plastic flow.
- Source extinction: This effect is common in nanocrystalline materials and is caused by a geometric constraint wherein small grains can only accommodate small dislocation loop diameters. As a result, extremely high local shear stresses are required to nucleate dislocations at a separation distance that is sufficient to avoid collapse of the dipole pair and cause immediate annihilation.

In the analysis of the two-dimensional domain shown in Figure 2, the material is assumed to be pure aluminum with monocrystalline square grains having side dimensions $h = w = 2.0$ μm , 1.0 μm , 0.5 μm , and 0.1 μm and is loaded uniaxially to 0.5% tensile strain in the y-direction. Elastic properties and the other parameters used in the DD simulation are listed in Table 1. Three slip planes were selected with orientations of 60, 0, -60 degrees. The choice of orientations is only constrained by rotation around an axis normal to a {111} plane in the FCC metal which defines a cut plane positioned to intersect three of the 12 available slip planes at an equal angle. This configuration is similar to the hexagonal crystal used in Miller (2004).

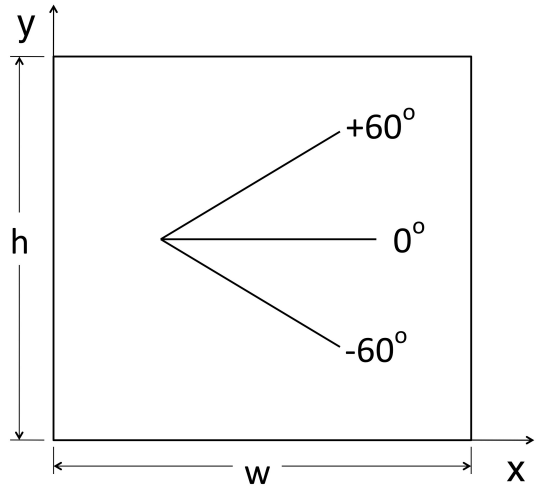

Figure 2: Model domain showing slip plane orientations.

Table 1.
Numerical constants, material properties, and load parameters for aluminum.

Parameter	Symbol	Value
Time step	Δt	0.25 ns
Shear modulus	μ	25.3 GPa
Poisson's ratio	ν	0.341
Burgers vector	b	0.285 nm
Source strength	τ_s	0.027 GPa
Obstacle strength	τ_o	0.08 GPa
Standard deviation	sd	0.2
Nucleation time	t_{nuc}	10.0 ns
Core diameter	c	6b nm
Capture distance	l_{cd}	6b nm
Slip plane separation	l_{slp}	100b
Velocity cut-off	v_{max}	100 m/s
Mobility factor	B	1.0×10^{-4} Pa s
Dynamic source probability	p_{ap}	0.04

In the present analysis, both dislocation pile-ups at the GB and pinning due to obstacles in the grain interior are simulated; however, nucleation of dislocations from the GB was not considered. A more complete discussion of options for considering grain boundaries in DD simulation is included in Appendix A. Each of the DD simulations was started with no pre-existing dislocations and with an identical initial source and obstacle density of $1.5 \times 10^{13}/m^2$. Various densities ranging from $5.0 \times 10^{12}/m^2$ to $1.0 \times 10^{14}/m^2$ were examined; the selected value represents a moderately low initial density but was found numerically adequate to demonstrate different grain behavior as a function of grain size over the range of interest.

The DD model must be free of finite edge effects in order to represent bulk material behavior and permit the DD simulation results to be mapped to a continuum crystal plasticity model. Hence, periodic boundary conditions (PBCs) are applied in which a central DD domain is replicated as image cells in both in-plane directions. If the assumed properties of the GBs permit dislocations to cross the boundary, they are modeled as reentering the cell on the opposite side. All images contribute to the stress calculation at dislocations in the central cell and the summation of stresses is carried out to a specified number of image layers. A schematic of the basic configuration used in applying PBCs is depicted in Figure 3, where the number of layers of image domains is determined through a convergence study of stress components at several locations in the model.

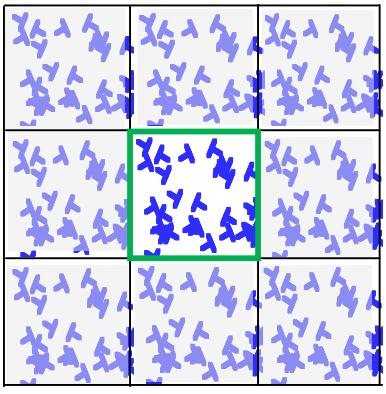

Figure 3: A central DD domain surrounded by periodic images to represent a boundary-free material.

An effective stress, $\bar{\sigma}_{yy}$, was determined by integrating the dislocation stress fields over the segment of the boundary at which an effective strain, $\bar{\varepsilon}_{yy}$, is applied. The resulting stress-strain response was computed using

$$\begin{aligned} \bar{\varepsilon}_{yy} &= \delta_y / h \\ \bar{\sigma}_{yy} &= \frac{1}{w}\int_0^w \sigma_{yy}(x)\,dx\Big|_{y=h} \end{aligned} \tag{1}$$

The stress-strain relations predicted by the simulation are presented in Figure 4a. Because of the constant mean source strength, all models exhibited a similar flow stress commencing at about 0.075% applied strain. This flow stress corresponds to the initiation of dislocation nucleation and begins when sources are subjected to a shear stress equal to or greater than the source strength of 27.0 MPa. Because no dislocations are initially present in the model, yield can only begin when this source strength is exceeded. After a source nucleates a dipole pair, it is required to remain dormant during the nucleation time of 10 ns. These and other parameters are listed in Table 1.

The observable trend from the DD analyses shows increasing hardening response with decreasing grain diameter. The response of the 0.1μm grain is essentially linear elastic for the selected source density. The 0.5μm grain exhibits distinct episodes of slip that result in a clear nonlinearity in stress-strain behavior. For the larger, 1.0μm and 2.0μm grains, stress-strain recovery shows a linear response until the initial nucleation of dislocations from sources followed by stress relief at approximately 0.1% strain. Similar simulation behavior showing stress relaxation has been presented elsewhere (Deshpande, 2001; Balint, 2006). After relaxation, depending on the specific material properties considered, the grain behavior either exhibits strain hardening with additional applied load or fluctuation about a constant stress state.

Figure 4b shows the resulting dislocation fields for the 0.5μm, 1.0μm, and 2.0μm grains at 0.5% strain. Few dislocations are nucleated in the 0.1μm x 0.1μm grains, thus their discussion is omitted. Dislocations are color coded in Figure 4b to indicate their distribution in the material domain: blue designates mobile dislocations, including those involved in pile-ups; purple indicates dislocations pinned due to interaction with obstacles or participation in junction formation; and red identifies dislocations that have exited the domain at the GB. The labels “A”, “B” and “C” on Figure 4a correspond to the same labels on Figure 4b to facilitate comparison between the stress-strain curves and the corresponding dislocation densities at 0.5% strain.

The dislocation profiles show that dislocation pile-ups occur both within the interior of the grain due to obstacles and along the GB. Once unpinned from an internal pile-up, dislocations may glide towards a GB where they may either participate in a GB pile-up or exit the domain. When dislocations exit the domain, their stress fields are set to zero and their displacement fields are maintained to preserve the simulated distortion of the material. Individual dislocations that become pinned at an obstacle but do not progress to a pile-up are also common. The effect of this type of trapping is similar to pile-up formation and produces hardening by preventing additional plastic slip due to dislocation glide in the grain interior.

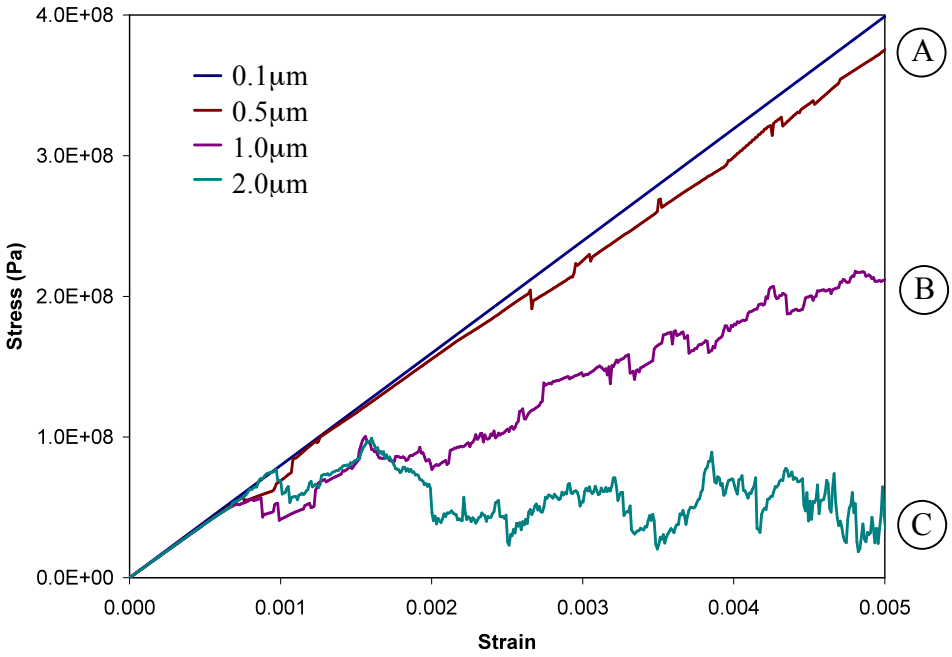

Figure 4a: Stress-strain response for 0.1μm, 0.5μm, 1.0μm, and 2.0μm grains.

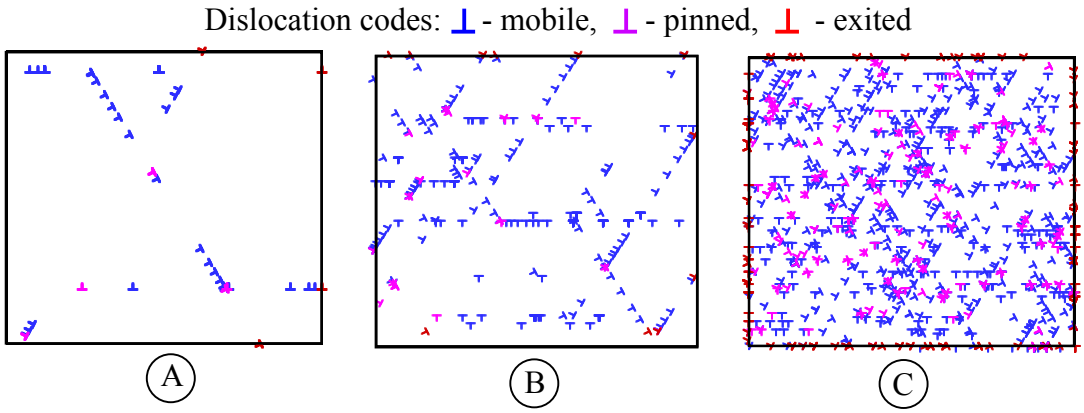

Figure 4b: Dislocation profile at 0.5% strain for the 0.5μm (A), 1.0μm (B) and 2.0μm (C) grains. Dislocations are classified as either mobile, pinned or exited.

Continuum Crystal Plasticity Formulation

An elastic-viscoplastic crystal plasticity formulation that follows the work of Matouš and Maniatty (Matouš, 2004) was implemented within a continuum finite element analysis. A brief overview of the CP constitutive model is given here, but is strictly limited to aspects that are

necessary for subsequent discussion. A recent review of crystal plasticity models can be found in Roters (2010).

The CP constitutive model is composed of a multiplicative decomposition of the total deformation gradient, F, into its elastic, F^e, and plastic parts, F^p. A power-law slip rate equation is used to determine the evolution of slip, $\dot{\gamma}^{\alpha}$, on the systems, α, given by

$$\dot{\gamma}^{\alpha} = \dot{\gamma}_o \frac{\tau^{\alpha}}{g^{\alpha}} \left| \frac{\tau^{\alpha}}{g^{\alpha}} \right|^{\frac{1}{m}-1} \tag{2}$$

where $\dot{\gamma}_o$ is the reference slip rate, τ^{α} is the resolved shear stress on system α, g^{α} is the current hardness on system α, and m, is a rate sensitivity parameter.

Hardness is represented by the Voce-Kocks hardening model and is computed as

$$\dot{g} = G_o \left(\frac{g_s - g}{g_s - g_o} \right) \dot{\gamma} \tag{3}$$

where G_o is a hardening rate parameter, g_o is the initial hardness, and g_s is the saturation value of the hardness. The Voce-Kocks hardening model enforces all slip systems to begin with the same hardness and subsequently harden at the same rate; consequently, the α superscripts have been dropped in Eq. 3. This hardening model has been used in previous crystal plasticity studies of Al polycrystal deformation (Matouš, 2004).

Multiscale Linking of DD and CP Simulations

In the present multiscale modeling method, crystal plasticity parameters are calibrated to the stress-strain behavior of a series of DD simulations having varying grain size to inform the multiscale DD/CP model. In mapping the higher fidelity results obtained from DD simulations to the lower fidelity continuum CP parameters, the reduced degree of representation that is available in the CP formulation yields an optimization problem in which the CP parameters are optimized to minimize the difference between the stress-strain predictions made by the DD/CP and DD models.

The Design Optimization Tools (DOT) library (DOT, 2011) was used to link a gradient-based optimization to a finite element simulation code. The finite element model was subjected to the same uniaxial loading as the DD model and was analyzed with free edge boundary conditions along x=0 and x=w in Figure 2. In the optimization procedure, the DD-simulated stress-strain behavior was used as the target solution and the CP parameters were varied until a minimum difference between the CP- and DD-predicted stress-strain curves was reached within a set tolerance. This process was repeated for each grain size.

The CP model of Matouš contains 15 material parameters that must be considered during the optimization. Three of the parameters are the Euler angles defining the grain orientation with respect to specimen coordinates and another three parameters are anisotropic elasticity constants. None of these six parameters are included in the optimization because they can be determined directly. Thus, nine parameters remain to capture various aspects of plastic hardening behavior. Two primary characteristics of plastic hardening behavior were observed to vary in the DD-predicted stress-strain behavior. The first characteristic is the initial hardening rate just after dislocation nucleation and is included in the analysis by calibration of the parameter g_o in Eq. 3. The second characteristic is the overall strain-hardening rate and is included in the analysis by calibration of the parameter G_o in Eq. 3. The remaining CP parameters were kept constant for all DD models since they were assumed to be independent of the grain size. Those values that were not optimized were set equal to values used in Matouš (2004) for pure aluminum.

The optimized parameters, G_o and g_o, are plotted as a logarithmic function of grain size, *h, w*, in Figure 5. The logarithmic equations fitted to the calibrated parameters can be used as input to the DD/CP polycrystal simulation, effectively incorporating the DD-predicted size-dependent stress-strain behavior. The resulting functional form is used to develop the DD/CP formulation and implicitly account for both the various mechanisms involved in the evolution of dislocations and the dynamic interactions of those dislocations.

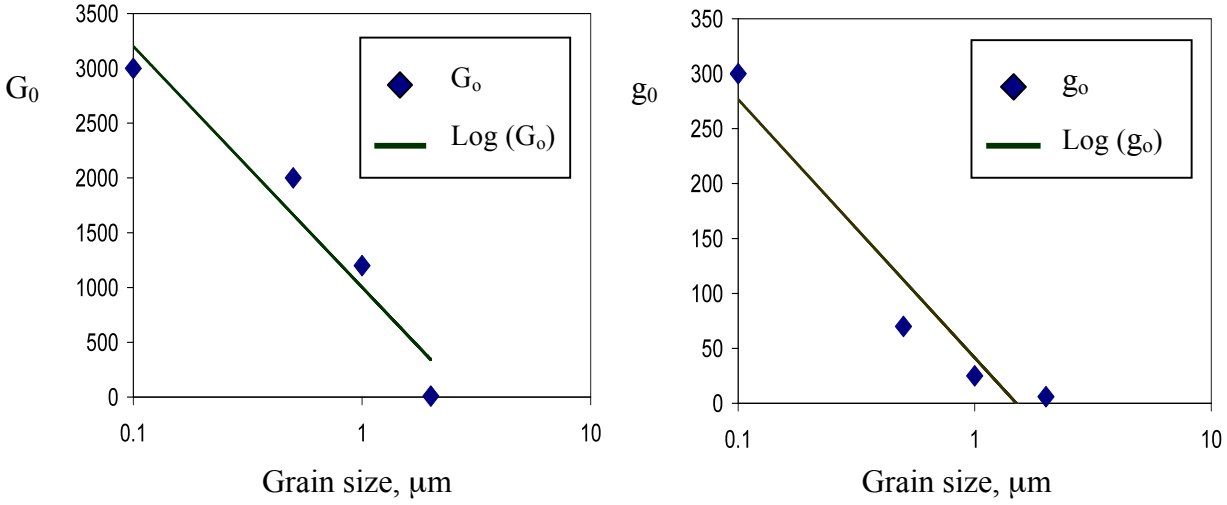

Figure 5: The calibrated functions G_o (left) and g_o (right) determining the evolution of hardness in DD/CP simulations.

The stress-strain curves from the DD simulation, shown in Figure 4a, are repeated as dashed lines in Figure 6 and then overlayed with the corresponding optimized DD/CP model analogues. The DD/CP model results for the square 0.1μm and 0.5μm grains are indistinguishable from the corresponding DD simulations. For the larger 1.0μm and 2.0μm grains that demonstrate a large degree of plasticity, the optimization of the DD/CP model parameters are necessarily constrained by the number of adjustable CP parameters and the mathematical forms of the governing CP

equations. The result is that the main features of the DD stress-strain relations, notably the flow stress, the slope of the hardening curve, and strain energy equal to the area under the curve, are represented in an averaged sense by the optimized DD/CP model. This averaged response is inherent to the multiscale analysis performed herein where the dynamic fluctuations of the DD stress-strain curves must be filtered or homogenized to extract the important features required for larger scale continuum analysis.

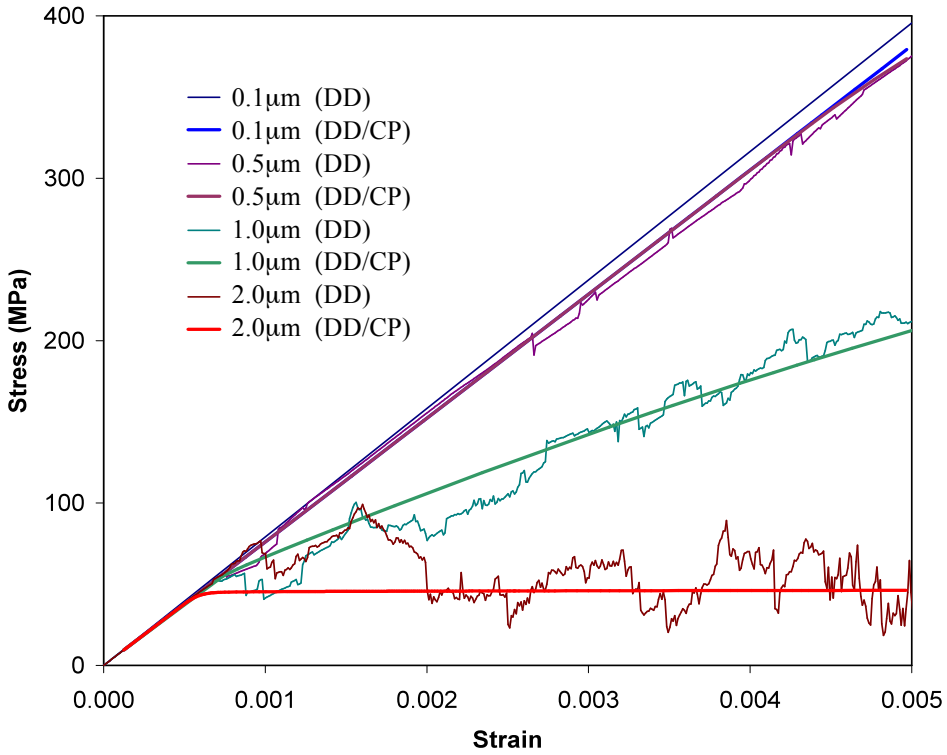

Figure 6: Comparison of stress-strain predictions using DD and the optimized DD/CP model.

Comparison of DD and CP Simulations of a Structurally-Graded Material Model

For simplicity, idealized square grains, as shown in Figure 7, were assumed to comprise the structurally-graded material. In addition, all grains were assumed to possess the same +60/0/-60 slip system and GBs were assigned reflective properties (see Appendix A). As a verification of the present approach, the configuration was simulated using both DD and the multiscale DD/CP model under uniaxial loading to 0.5% strain in the *y*-direction. The DD model of the structurally-graded material was simulated using PBCs only in the vertical direction to remove edge effects on the top and bottom surfaces and free edge conditions on the left and right surfaces to preserve the effect of grading the grain dimensions in the *x*-direction. If PBCs were introduced on the left and right surfaces, images that cause the smallest grains on the right to be influenced by an adjacent image of the largest grain on the left would have been produced. The DD/CP model of the structurally-graded material was simulated under plane-strain conditions with CP parameters that were obtained using the results of the fully periodic single grain DD simulations.

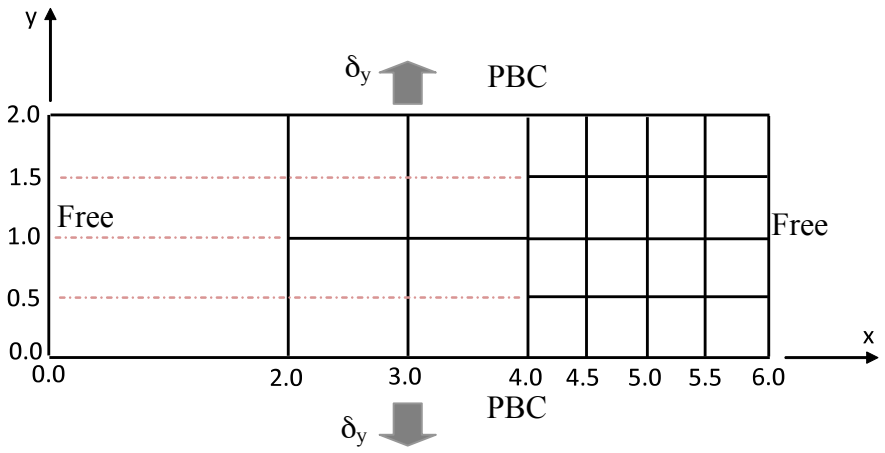

Figure 7: Structurally-graded polycrystal model containing 2.0μm, 1.0μm , and 0.5μm square grains. Boundary conditions applied to model faces are identified as Free or PBC. All model dimensions are in microns.

The effective stress is obtained by applying Eq. 1 for each grain along the outer boundary and averaging along the length of the model. The computation of effective stress becomes

$$\bar{\sigma}_{yy} = \frac{1}{L}\left[\sum_{i}^{N} l_i \int_{L_{i-1}}^{L_i} \sigma_{yy} dx\right] = \frac{1}{L}\left[\sum_{i}^{N} l_i \bar{\sigma}_{yy,i}\right] \tag{4}$$

where N is the number of boundary grains, L is the total length given by the sum of individual grain lengths, l_i, along the outer boundary as

$$L = \sum_{i}^{N} l_i \tag{5}$$

Figure 8 shows the stress-strain results of the DD simulation and the DD/CP model. The DD simulation predicts a peak stress of about 60 MPa followed by an immediate drop in stress and a subsequent hardening. This local peak after initial yield has been observed by other authors (see, for example, Despande, 2001; Balint, 2006) and is believed to occur because the applied strain rate of 4.0×10^4 s^{-1} in the DD simulation does not allow sufficiently rapid dislocation nucleation to immediately soften the material.

As seen in the figure, the DD/CP model follows the DD predictions closely up to the first peak at a stress of approximately 60 MPa and then follows a strain hardening path that is parallel but somewhat offset from the DD results. An examination of Eq. 3 shows that the CP hardening equation used in the DD/CP model cannot represent the localized drop in stress as predicted by the DD results. Thus, the discrepancy between the DD and DD/CP curves is believed to be the

result of a combination of the strain rate in the DD simulation and the inability of the DD/CP model to represent non-monotonic softening.

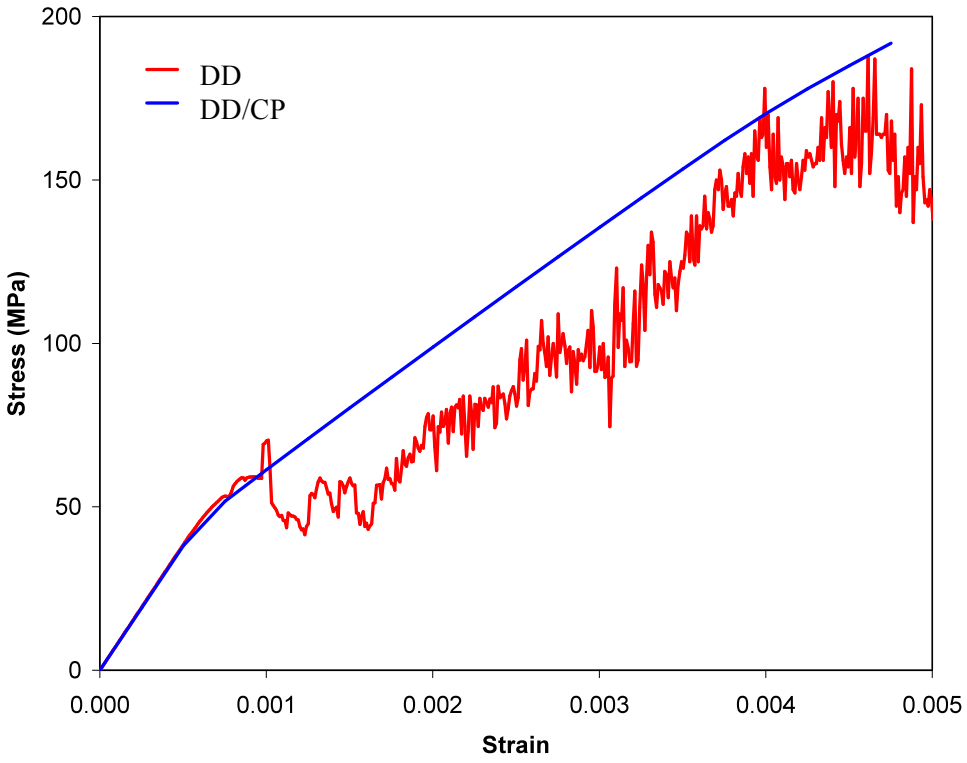

Figure 8: Comparison of DD- and DD/CP-predicted stress-strain behavior in the structurally-graded polycrystal model.

Summary

A multiscale modeling method has been developed that integrates discrete dislocation plasticity with continuum crystal plasticity to enable the analysis of structurally-graded metallic materials having grain sizes that range from about a hundred nanometers to several microns. This multiscale method is aimed at representing the detailed deformation mechanisms determined by discrete dislocation dynamics, including dislocation nucleation, glide, annihilation, pinning and pile-up, within computationally efficient continuum crystal plasticity (CP) analyses.

A discussion of two-dimensional discrete dislocation (DD) methods was presented together with their application to the study of the effects of grain size on deformation. The effect of grain size was demonstrated by showing simulated stress-strain predictions exhibiting a range of stress-strain response from nearly linear elastic to nearly elastic-perfectly plastic as the grain size increased from 0.1μm to 2.0 μm. In these simulations, both the initial source density and obstacle density were fixed at $1.5 \times 10^{13}/m^2$.

The optimization procedure that was used to calibrate CP hardening parameters and develop a dislocation-based crystal plasticity model (the DD/CP model) from the DD simulations was outlined. The main features of the DD stress-strain relations were represented in an averaged sense by the optimized DD/CP model. The results of a verification problem, where the stress-strain behavior of a structurally-graded polycrystal was predicted separately using DD simulation and the DD/CP model, were presented. Both the ability of the DD/CP model to reproduce the trends of the DD simulation and its inability to capture the rate-dependent stress relaxation seen in the DD simulation were also discussed.

Appendix A: Simulation of Grain Boundaries

The range of different atomic structures comprising GBs in metallic materials is large and significantly affects the energetics of the dislocation-GB interactions. The interactions occur through a variety of mechanisms that must be considered in the DD simulations. Dislocation-GB interactions can be represented by a combination of reflection, absorption, and transmittance (Shen, 1988) in DD analyses as depicted in Figure A1.

In DD analysis, reflection can be simulated by preventing dislocations from crossing a GB and allowing them to freely glide away at a pre-determined incident angle. Absorption can be simulated by pinning dislocations at the GB. Transmittance can be simulated by allowing dislocations to exit the material domain when crossing an external boundary or allowing them to enter an adjacent grain when crossing an internal boundary in a polycrystal model. Dislocations that have exited the material domain are held at the boundary, although their stress fields are set to zero. For dislocations transmitted across a GB into a neighboring grain, the placement within the new slip system is made such that the change in angle between the original and new slip plane is a minimum (Clark, 1992). In the present work, GB properties were assumed to be reflective.

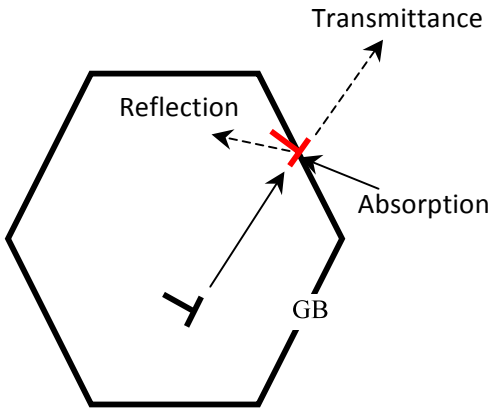

Figure A1: Dislocation – GB interactions.

The elastic properties of grain boundaries have been recently shown to have significant spatial variation on an atomistic scale (Adams, 1989; Schiotz, 1999; Wolf, 1993). However, the thickness, $t_{GB,}$ of a GB is very small (on the order of 1 nm). Additionally, surrounding grains in a polycrystal enforce strong kinematic constraints. Thus, both normal and shear stress components are assumed to be fully transmitted across GBs and the summation of long-range stresses on objects in one grain from dislocations in surrounding grains is assumed to be negligibly affected by the presence of interposed GBs.

Acknowledgements

This work was supported by the NASA Aeronautics Research Mission Directorate Seedling Fund for early-stage innovation.

References

Adams, J.B., Wolfer, W.G., and Foiles, S.M., "Elastic Properties of Grain Boundaries in Copper and Their Relationship to Bulk Elastic Constants," *Phys. Rev. B*, Vol. 40, 1989, pp. 9479-9484.

Benzerga, A.A., Brechet, Y., Needleman, A., and Van der Giessen, E., "Incorporating Three-Dimensional Mechanisms into Two-Dimensional Dislocation Dynamics*, Modelling Simul. Mater. Sci. Eng.*, Vol. 12, 2004, pp.159-196.

Balint, D.S., Deshpande, V.S., Needleman, A., and Van der Giessen, E., "Size Effects in Uniaxial Deformation of Single and Polycrystals: A Discrete Dislocation Plasticity Analysis," *Modelling Simul. Mater. Sci. Eng.*, Vol. 14, 2006, pp. 409-423.

Clark, W.A.T., Wagoner, R.H., Shen, Z.Y., Lee, T.C., Robertson, I.M., and Birnbaum, H.K., "On the Criteria for Slip Transmission Across Interfaces in Polycrystals," *Scripta Metall. Mater*., Vol. 26, 1992, pp. 203-206.

Deshpande, V.S., Needleman, A., and Van der Giessen, E., "Dislocation Dynamics is Chaotic," *Scripta Mater.*, Vol. 45, 2001, pp. 1047-1053.

Deshpande, V.S., Needleman, A., and Van der Giessen, E., "Discrete Dislocation Plasticity Modeling of Short Cracks in Single Crystals," *Acta Mater.*, Vol. 51, 2003, pp.1-15.

Devincre, B., Kubin, L.P., Lemarchand, C., and Madec, R., "Mesoscopic Simulations of Plastic Deformation," *Mat. Sci. Eng.*, Vol. A309-310, 2001, pp. 211-219.

DOT library, ref[http://www.vrand.com/DOT.html]

Evans, A.G. and Hutchinson, J.W., "A Critical Assessment of Theories of Strain Gradient Plasticity," *Acta Mater.*, Vol. 57, 2009, pp. 1675-1688.

Evers, L.P., Parks, D.M., Brekelmans, W.A.M., and Geers, M.G.D., "Crystal Plasticity Model with Enhanced Hardening by Geometrically Necessary Dislocation Accumulation," *J. Mech. Phys. Solids*, Vol. 50, 2002, pp. 2403-2424.

Fang, T.H., Li, W.L., Tao, N.R., and Lu, K., "Revealing Extraordinary Intrinsic Tensile Plasticity in Gradient Nano-Grained Copper," *Science*, Vol. 331, 2011, pp. 1587-1590.

Fleck, N.A., Muller, G.M., Ashby, M.F. and Hutchinson, J.W., "Strain Gradient Plasticity: Theory and Experiment," *Acta Metall. Mater.*, Vol. 42, No. 2, 1994, pp. 475-487.

Fleck, N.A. and Hutchinson, J.W., "Strain Gradient Plasticity," *Adv. in Appl. Mech.*, Vol. 33, 1997, pp. 295-361.

Freidman, L.H. and Chrzan, D.C., "Scaling Theory of the Hall-Petch Relation for Multilayers," *Phys. Rev. Lett.*, Vol. 81, 1998, pp. 2715-2718.

Gavriljuk, V.G., Berns, H., Escher, C., Glavatskaya, N.I., Sozinov, A., and Petrov, Y.N., "Grain Boundary Strengthening in Austenitic Nitrogen Steels," *Mat. Sci. Eng.*, Vol. 271, 1999, pp. 14-21.

Gleiter, H., "Nanocrystalline Materials," *Prog. Matl. Sci.*, Vol. 33, 1989, pp. 223-315.

Hall, E.O., "The Deformation and Ageing of Mild Steel: III Discussion of Results," *Proc. Phys. Soc.*, Ser. B, Vol. 64, 1951, pp. 747-753.

Han, C.-S., Gao, H., Huang, Y., and Nix, W., "Mechanism-Based Strain Gradient Crystal Plasticity-I. Theory," *J. Mech. Phys. Solids*, Vol. 53, 2005, pp. 1188-1203.

Han, C.-S., Gao, H., Huang, Y., and Nix, W., "Mechanism-Based Strain Gradient Crystal Plasticity-II. Analysis," *J. Mech. Phys. Solids*, Vol. 53, 2005, pp. 1204-1222.

Ho Oh, S., Legros, M., Kiener, D., and Dehm, G., "In Situ Observation of Dislocation Nucleation and Escape in a Submicrometre Aluminum Single Crystal," *Nature Materials*, Vol. 8., 2009, pp. 95-100.

Hull, D. and Bacon, D.J., *Introduction to Dislocations*, Butterworth-Heinemann, Oxford, 2001.

Hutchinson, J.W., "Plasticity at the Micron Scale," *Int. J. Solids and Struct.*, Vol. 37, 2000, pp. 225-238.

Li, J.C.M. and Cho, Y.T., "The Role of Dislocations in the Flow Stress-Grain Size Relationships," *Metall. Trans.*, Vol. 1, 1970, pp. 1145–1159.

Matouš, K. and Maniatty, A.M., "Finite Element Formulation for Modeling Large Deformations in Elasto-Viscoplastic Polycrystals," *Int. J. Num. Meth. Engrg.*, Vol. 60, 2004, pp. 2313-2333.

Miller, R.E., Shilkrot, L.E., and Curtin, W.A., "Coupled Atomistics and Discrete Dislocation Plasticity Simulation of Nanoindentation into Single Crystal Thin Films," *Acta Mater.*, Vol. 52, 2004, pp. 271-284.

Mughrabi, H., "Dislocation Wall and Cell Structures and Long-Range Internal Stresses in Deformed Metal Crystal," *Acta Metall.*, Vol. 31, 1983, pp.1367-1379.

Needleman, A. and Van der Giessen, E., "Micromechanics of Fracture: Connecting Physics to Engineering," *MRS Bulletin*, March 2001, pp. 211-214.

Petch, N.J., *J.* "The Cleavage Strength of Polycristals," *Iron and Steel Institute*, 1953, pp. 25-28.

Qin, K., Yang, L., and Hu, S., "Mechanism of Strain Rate Effect Based on Dislocation Theory," *Chin. Phys. Lett.*, Vol. 26, 2009, p. 036103.

Ross, A., De Hosson, J.Th.M., and Van Der Giessen, E., "High-Speed Dislocations in High Strain-Rate Deformations," *Comp. Mat. Sci.*, Vol. 20, 2001, pp.19-27.

Roters, F., Eisenlohr, P., Hantcherli, L., Tjahjanto, D.D., Bieler, T.R., and Raabe, D., "Overview of Constitutive Laws, Kinematics, Homogenization and Multiscale Methods in Crystal Plasticity Finite-Element Modeling: Theory, Experiments, Applications," *Acta Mater.*, Vol. 58, 2010, pp. 1152-1211.

Saether, E., Yamakov, V., Phillips, D.R., and Glaessgen, E.H., "An Overview of the State of the Art in Atomistic and Multiscale Simulation of Fracture," NASA TM-2009-215564, 2009.

Schiotz, J., Vegge, T., Di Tolla, F.D., and Jacobsen, K.W., "Atomic-Scale Simulations of the Mechanical Deformation of Nanocrystalline Metals," *Phys. Rev. B*, Vol. 60, 1999, pp. 11971-11983.

Shen, Z., Wagoner, R.H., and Clark, W.A.T., "Dislocation and Grain Boundary Interactions in Metals," *Acta Metall*., Vol. 36, 1988, pp. 3231-3242.

Thomson, R., Levine, L.E., Shim, Y., Savage, M.F., and Kramer, D.E., "A Multi-Scale Theoretical Scheme for Metal Deformation," *Comp. Model. Engr. Sci.*, Vol. 3, 2002, pp. 245-253.

Uchic, M.D., Shade, P.A., and Dimiduk, D.M., "Plasticity of Micrometer-Scale Single Crystal in Compression," *Ann. Rev. Mater. Res.*, Vol. 39, 2009, pp. 361-386.

Van der Giessen, E., and Needleman, A., Discrete Dislocation Plasticity: A Simple Planar Model," *Modelling Simul. Mater. Sci. Eng.*, Vol. 3 (1995), pp. 689-735.

Warner, 2007: Warner, D. H., Curtin, W. A., and Qu, S., "Rate Dependence of Crack-Tip Processes Predicts Twinning Trends in f.c.c. Metals," *Nature Mater.*, vol. 6, 2007, pp. 876-880.

Whang, S.H., *Nanostructured Metals and Alloys: Processing, Microstructure, Mechanical Properties and Applications*, Woodhead Publishing, Oxford, 2011.

Wolf, D. and Jaszczak, J.A., "Tailored Elastic Behavior of Multilayers through Controlled Interface Structure," *J. Computer-Aided Design*, Vol. 1, 1993, pp. 111-148.

Yamakov, V., Saether, E., Phillips, D. R., and Glaessgen, E. H., "Molecular-Dynamics Simulation-Based Cohesive Zone Representation of Intergranular Fracture Processes in Aluminum," *J. Mech. Phys. Solids*, 54, 2006, pp. 1899-1928.

Yamakov, V., Saether, E., and Glaessgen, E.H., "A Continuum-Atomistic Analysis of Transgranular Crack Propagation in Aluminum," 50th AIAA/ASME/ASCE/AHS/ASC Structures, Structural Dynamics and Materials Conference and Exhibit, Palm Springs, CA, 2009.

Zhu, B., Asaro, R.J., Krysl, P., Zhang, K., and Weertman, J.R., "Effects of Grain Size Distribution on the Mechanical Response of Nanocrystalline Metals: Part II," *Acta Mater.*, Vol. 54, 2006, pp. 3307-3320.